DISTRIBUTED CLOCK SYNCHRONIZATION AND RANGING IN TIME-VARIANT WIRELESS NETWORKS

Daniel Bartel *Bernhard Etzlinger* *Andreas Springer*

Institute of Communications Engineering and RF-Systems
Johannes Kepler University Linz, Austria
Email: {d.bartel, b.etzlinger, a.springer}@nthfs.jku.at

ABSTRACT

Clock synchronization and ranging are important topics in the field of wireless networks, where internode time measurement allows both tasks to be completed in one. Such networks are generally time-variant due to possible changes in environmental conditions and mobility of network nodes. We present a fully distributed filtering algorithm for combined clock synchronization and ranging based on message passing by belief propagation on a factor graph representation of a time-variant wireless network. The resulting message passing equations can be interpreted as a variant of Kalman filtering locally on each network node. Simulation results show that tracking estimation parameters improves estimation accuracy significantly without additional communication effort.

Index Terms— Clock synchronization, ranging, belief propagation, factor graphs, Kalman filtering

1. INTRODUCTION

In wireless networks (WNs), a shared notion of time is a fundamental requirement in a variety of tasks [1–3]. In addition, emerging application areas require internode distance estimation [4–6], also referred to as ranging. Clock synchronization can be seen as the key to achieving a shared notion of time. Considering that neighboring nodes of a WN share timing information by a two-way packet exchange mechanism [7], a relationship exists between the line-of-sight propagation delay of packets and internode distances.

There is a recent trend towards clock synchronization by means of probabilistic graphical models, i. e., factor graphs (FGs) [8]. This method offers fully distributed algorithms that lead to better scalability, since the same algorithm is executed on each node. Introduced by [9], belief propagation (BP) is used for distributed clock offset synchronization in a WN.

Individual nodes usually acquire their knowledge of time from local clocks, for instance, oscillators. However, these are affected by hardware imperfections [10, 11] that cause time drifts between local clocks. In order to avoid frequent resynchronization procedures for drift compensation, an extension of the FG approach in [9] that offers combined estimation of both clock skew and offset was proposed in [12, 13]. On the basis of [13], a distributed synchronization and ranging algorithm has recently been introduced in [14], where a time-invariant WN has been assumed.

In general, clock parameters and internode distances are time-variant due to possible changes in environmental conditions and mobility of nodes. If the parameters of a WN change over time, the above-mentioned methods require re-estimation in each synchronization period using a new set of measurements, which ignores dependencies between the synchronization periods. Therefore, tracking the time-variant parameters improves estimation accuracy. Solutions using FGs for time-variant clock offset estimation between two nodes have recently been introduced in [15, 16]. Another approach based on the Expectation-Maximation algorithm that performs clock synchronization and localization for time-varying clock parameters was presented in [17]. The method is limited to a single pair of nodes, and network-wide distance estimation via localization is computationally demanding. To the best of our knowledge, no fully distributed algorithm for combined network-wide time-variant clock synchronization and ranging is available.

The work presented here focuses on the extension of combined clock synchronization and ranging to WNs, which are time-variant in both clock parameters and distances. Our algorithm combines clock skew and offset estimation with ranging by using a distributed filtering approach. It enables distributed tracking of time-varying parameters on each node of a WN. Its derivation is based on BP message passing on an FG representing a time-variant WN. Simulation results show that considering dependencies between synchronization periods leads to an improvement in estimation accuracy.

2. SYSTEM MODEL

Similar to [14], a WN of N nodes is considered, where a node $i \in \mathcal{I} \triangleq \{1, \ldots, N\}$ belongs either to a subset $\mathcal{M}$ of synchronous master nodes or a subset $\mathcal{A}$ of asynchronous agent nodes, meaning that $\mathcal{I} = \mathcal{M} \cup \mathcal{A}$. Each node i possesses a local clock time

$$c_i(t) = \alpha_i(t)\, t + \beta_i, \tag{1}$$

where $\alpha_i(t)$ denotes the time-variant local clock skew and β_i the time-invariant local clock phase. If $i \in \mathcal{M}$, it is assumed that $\alpha_i(t) = 1$ and $\beta_i = 0$. The time-variant distance between node $i \in \mathcal{I}$ and a node $j \in \mathcal{I}$ is given as $d_{ij}(t) = d_{ji}(t)$. If $d_{ij}(t) < R$, the node pair (i, j) can communicate with each other, and R denotes the corresponding communication range. The tupel (i, j) is then added to the connection set $\mathcal{C}$, and the set of all neighbors of a node $i \in \mathcal{I}$ is given as $\mathcal{T}_i \triangleq \{j \in \mathcal{I} \,|\, (i, j) \in \mathcal{C}\}$.

As in [13], nodes exchange information by means of packets during a measurement period T_l and a subsequent message passing period T_m. Both periods are repeated with the synchronization period T_n, and therefore $T_n \geq T_l + T_m$. We approximate the time-variant parameters $\alpha_i(t)$ and $d_{ij}(t)$ as piecewise constant functions with interval T_n. This leads to an approximation

$$\alpha_i(t) \approx \sum_{n=0}^{\infty} \alpha_{i,n}\, \mathrm{rect}\left(\frac{t - (n + \frac{1}{2})T_n}{T_n}\right) \tag{2}$$

978-1-4799-2893-4/14/$31.00 ©2014 IEEE

with $\alpha_{i,n} \triangleq \alpha_i(nT_n)$ and an analogous approximation $d_{ij}(t)$ with $d_{ij,n} \triangleq d_{ij}(nT_n)$. In order to compensate for clock errors introduced by (2), β_i must also be modeled as a piecewise constant function [17], which yields $\beta_{i,n}$. To capture time-variations, a Gauss-Markov evolution model is used for $\alpha_{i,n}$, $\beta_{i,n}$, and $d_{ij,n}$. We can thus write, for example, for $\alpha_{i,n}$ (and analogously for $\beta_{i,n}$ and $d_{ij,n}$):

$$\alpha_{i,n} = \alpha_{i,n-1} + u_n, \tag{3}$$

where $u_n \overset{iid}{\sim} \mathcal{N}_u(0, \sigma_u^2)$. For mathematical simplicity, we assume σ_u^2 to be equal for all three parameters.

In order to perform clock synchronization and ranging, the pairwise exchange of time stamps is applied across the network [7]. If $(i,j) \in \mathcal{C}$, node i transmits $K_{ij} \geq 1$ packets to node j and receives $K_{ji} \geq 1$ packets from node j. The k-th packet from node i is transmitted at send time $s_{ij,n}^{(k)}$ and received by node j at receive time $r_{ij,n}^{(k)} = t_{ij,n}^{(k)} + \delta_{ij,n}^{(k)}$. The line-of-sight propagation delay is

$$\delta_{ij,n}^{(k)} = d_{ij,n}/v_0 + w_{ij,n}^{(k)} \tag{4}$$

with the propagation velocity v_0 and $w_{ij,n}^{(k)} \overset{iid}{\sim} \mathcal{N}_w(0, \sigma_w^2)$ being Gaussian measurement noise. The send and receive times are recorded in local time as time stamps: $c_{i,n}(s_{ij,n}^{(k)})$ and $c_{j,n}(r_{ij,n}^{(k)})$. By considering (1), the relation between transmitted and received time stamps can be written as

$$c_{j,n}(r_{ij,n}^{(k)}) = \frac{c_{i,n}(s_{ij,n}^{(k)}) - \beta_{i,n}}{\alpha_{i,n}}\alpha_{j,n} + \beta_{j,n} + \frac{d_{ij,n}}{v_0}\alpha_{j,n} + w_{ij,n}^{(k)}\alpha_{j,n}, \tag{5}$$

for $k \in \{1, \ldots, K_{ij}\}$. A similar relation holds for the packets sent by node j to node i by exchanging i and j in (5). It is assumed that the time stamps $c_{i,n}(s_{ij,n}^{(k)})$ and $c_{i,n}(r_{ji,n}^{(k)})$ are recorded precisely. The aggregated observation between nodes i and j in the n-th synchronization period is given by [17] as

$$\mathbf{c}_{ij,n} = [\mathbf{c}_{i\to j,n}^{\mathrm{T}}, -\tilde{\mathbf{c}}_{j\to i,n}^{\mathrm{T}}]^{\mathrm{T}}, \tag{6}$$

with the vector of received time stamps

$$\mathbf{c}_{i\to j,n} \triangleq \left[c_{j,n}(r_{ij,n}^{(1)}), c_{j,n}(r_{ij,n}^{(2)}), \ldots, c_{j,n}(r_{ij,n}^{(K_{ij})})\right]^{\mathrm{T}}$$

and the vector of transmitted time stamps

$$\tilde{\mathbf{c}}_{j\to i,n} \triangleq \left[c_{j,n}(s_{ji,n}^{(1)}), c_{j,n}(s_{ji,n}^{(2)}), \ldots, c_{j,n}(s_{ji,n}^{(K_{ji})})\right]^{\mathrm{T}}.$$

Finally, all observations $\mathbf{c}_{ij,n}$ of all nodes $\mathcal{I}$ are stacked into $\mathbf{c}_n$, and all distances $d_{ij,n}$ into $\mathbf{d}_n$. The clock parameters $\boldsymbol{\theta}_{i,n} = [\alpha_{i,n}, \beta_{i,n}]^{\mathrm{T}}$ are hereafter treated in the form of transformed clock parameters $\boldsymbol{\vartheta}_{i,n} = [\lambda_{i,n}, \chi_{i,n}]^{\mathrm{T}} \triangleq [1/\alpha_{i,n}, \beta_{i,n}/\alpha_{i,n}]^{\mathrm{T}}$. Additionally, the following notation will be convenient: $\mathbf{r}_{ij,n} = [\mathbf{r}_{i,n}^{\mathrm{T}}, \mathbf{r}_{j,n}^{\mathrm{T}}]^{\mathrm{T}}$ and $\mathbf{r}_n = [\mathbf{r}_{1,n}^{\mathrm{T}}, \ldots, \mathbf{r}_{N,n}^{\mathrm{T}}]^{\mathrm{T}}$ for $\mathbf{r} \in \{\boldsymbol{\theta}, \boldsymbol{\vartheta}\}$.

3. STATISTICAL MODEL

In each measurement period T_l, the observations $\mathbf{c}_{ij,n}$ for a pair of nodes $(i,j) \in \mathcal{C}$ form a local likelihood function that can be derived from (5) by using an approximation as in [13]:

$$p(\mathbf{c}_{ij,n}|\boldsymbol{\vartheta}_{ij,n}, d_{ij,n}) \propto \exp\left(-\frac{\|\mathbf{A}_{ij,n}\boldsymbol{\vartheta}_{i,n} + \mathbf{B}_{ij,n}\boldsymbol{\vartheta}_{j,n} + \mathbf{a}_d d_{ij,n}\|^2}{2\sigma_w^2}\right) \tag{7}$$

with

$$\mathbf{A}_{ij,n} \triangleq \begin{bmatrix} -\tilde{\mathbf{c}}_{i\to j,n} & \mathbf{1}_{K_{ij}} \\ \mathbf{c}_{j\to i,n} & -\mathbf{1}_{K_{ji}} \end{bmatrix}, \quad \mathbf{B}_{ij,n} \triangleq \begin{bmatrix} \mathbf{c}_{i\to j,n} & -\mathbf{1}_{K_{ij}} \\ -\tilde{\mathbf{c}}_{j\to i,n} & \mathbf{1}_{K_{ji}} \end{bmatrix},$$

and $\mathbf{a}_d \triangleq -\frac{1}{v_0}\mathbf{1}_{K_{ij}+K_{ji}}$, where $\mathbf{1}_S$ denotes a column vector of size S filled with ones. Note that (7) is a member of the exponential family [18]. Further, if node $i \in \mathcal{I}$ has perfect knowledge of the transformed clock parameters $\boldsymbol{\vartheta}_{j,n}$ of node j and the distance $d_{ij,n}$ with $j \in \mathcal{T}_i$, then (7) can be written as a Gaussian emission distribution

$$p(\mathbf{c}_{ij,n}|\boldsymbol{\vartheta}_{ij,n}, d_{ij,n}) = \mathcal{N}_{\mathbf{y}_{i,n}}\left(-\mathbf{A}_{ij,n}\boldsymbol{\vartheta}_{i,n}, \sigma_w^2\mathbf{I}_{K_{ij}+K_{ji}}\right), \tag{8}$$

where $\mathbf{y}_{i,n} \triangleq \mathbf{B}_{ij,n}\boldsymbol{\vartheta}_{j,n} + \mathbf{a}_d d_{ij,n}$ can be interpreted as modified observations, and $\mathbf{I}_S$ denotes an identity matrix of size S. By assuming conditionally independent obervations, the network-wide likelihood function is given as

$$p(\mathbf{c}_n|\boldsymbol{\vartheta}_n, \mathbf{d}_n) = \prod_{(i,j)\in\mathcal{C}} p(\mathbf{c}_{ij,n}|\boldsymbol{\vartheta}_{ij,n}, d_{ij,n}). \tag{9}$$

In addition to the likelihood function obtained through measurements, each node $i \in \mathcal{I}$ has prior knowledge of its local transformed clock parameters $\boldsymbol{\vartheta}_{i,n}$ and its distances d_{ij} with $j \in \mathcal{T}_i$. For master nodes $i \in \mathcal{M}$, perfect prior knowledge is available, i. e., $p(\boldsymbol{\vartheta}_{i,0}) = \delta(\boldsymbol{\vartheta}_{i,0} - \bar{\boldsymbol{\vartheta}}_{i,0})$, where $\bar{\boldsymbol{\vartheta}}_{i,0}$ denotes the true transformed clock parameter of i and $\delta(\cdot)$ the Dirac delta function. For agent nodes $i \in \mathcal{A}$, the prior function is $p(\boldsymbol{\vartheta}_{i,0}) = \mathcal{N}_{\boldsymbol{\vartheta}}(\boldsymbol{\mu}_{\mathrm{p},i}, \boldsymbol{\Sigma}_{\mathrm{p},i})$ with $\boldsymbol{\mu}_{\mathrm{p},i} = [1\ \ 0]^{\mathrm{T}}$ and $\boldsymbol{\Sigma}_{\mathrm{p},i} = \mathrm{diag}\{\sigma_{\lambda_i}^2, \sigma_{\chi_i}^2\}$. The uncertainty over the local clock skew is captured by $\sigma_{\lambda_i}^2$, which is typically given by the clock specifications. In order to model the absence of prior knowledge of the local clock phase, a large value is usually chosen for $\sigma_{\chi_i}^2$. A prior function on the distance $p(d_{ij,0})$ can further be assumed and depends on the topology of the WN. For efficient algorithm design, a Gaussian representation $p(d_{ij,0}) = \mathcal{N}_d(\mu_{\mathrm{p},ij}, \Sigma_{\mathrm{p},ij})$ is chosen. Assuming that all local prior functions are statistically independent, the network-wide prior function is given as

$$p(\boldsymbol{\vartheta}_0, \mathbf{d}_0) = \prod_{(i,j)\in\mathcal{C}} p(d_{ij,0}) \prod_{i\in\mathcal{I}} p(\boldsymbol{\vartheta}_{i,0}). \tag{10}$$

Additionally, a network-wide transition function for $\boldsymbol{\vartheta}_n$ is derived from the Gauss-Markov evolution models of $\alpha_{i,n}$ and $\beta_{i,n}$ as

$$p(\boldsymbol{\vartheta}_n|\boldsymbol{\vartheta}_{n-1}) = \prod_{i\in\mathcal{M}} \delta(\boldsymbol{\vartheta}_{i,n} - \boldsymbol{\vartheta}_{i,n-1}) \prod_{i\in\mathcal{A}} \mathcal{N}_{\boldsymbol{\vartheta}_{i,n}}(\boldsymbol{\vartheta}_{i,n-1}, \sigma_u^2\mathbf{I}_2) \tag{11}$$

and similarly for $\mathbf{d}_n$. The likelihood function (9), the prior function (10), and the transition functions are subsequently used to formulate a distributed filtering algorithm for clock synchronization and ranging in time-variant WNs.

4. DISTRIBUTED FILTERING

The goal is to obtain in every synchronization period T_n a minimum mean square error (MMSE) estimate for the unknown parameters $\boldsymbol{\vartheta}_{i,n}$ and $d_{ij,n}$ with $j \in \mathcal{T}_i$ of each node $i \in \mathcal{A}$. The system model of section 2 can be written as a nonlinear filtering problem in the form of a discrete-time state-space model given as

$$\mathbf{x}_n = \mathbf{G}\,\mathbf{x}_{n-1} + \mathbf{v}_n \tag{12a}$$

$$\mathbf{y}_n = h(\mathbf{x}_n, \mathbf{w}_n), \tag{12b}$$

where $\mathbf{x}_n \triangleq [\boldsymbol{\vartheta}_n^{\mathrm{T}}, \mathbf{d}_n^{\mathrm{T}}]^{\mathrm{T}}$, $\mathbf{y}_n \triangleq \mathbf{c}_n$, $\mathbf{v}_n$, and $\mathbf{w}_n$ are the n-th state, observation, process noise, and observation noise variables, respectively, with respect to the unknown state $\mathbf{x}_n$. The initial state $\mathbf{x}_0$ is determined by the given prior function (10). Furthermore, $\mathbf{v}_n$ and $\mathbf{w}_n$ are assumed to be independent white Gaussian noise sequences

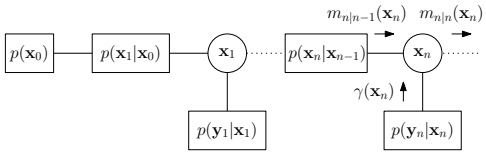

Fig. 1. Factor graph of the global posterior function (13); factor vertices f_i are shown as rectangles and variable vertices v_i are shown as circles.

with $\mathbf{v}_n \sim \mathcal{N}_{\mathbf{v}}(0, \mathbf{\Gamma})$ and $\mathbf{w}_n \sim \mathcal{N}_{\mathbf{w}}(0, \sigma_w^2 \mathbf{I}_{|\mathcal{C}|})$, where $\mathbf{\Gamma}$ is derived from (11). In (12), the matrix $\mathbf{G} = \mathbf{I}_{2|\mathcal{I}|+|\mathcal{C}|}$ is called transition matrix, and $h(\cdot)$ is the vector form of the nonlinear measurement equation (5). Based on (9) and (11), the state-space model of (12) can be written in terms of transition and emission distributions as

$$\begin{aligned} p(\mathbf{x}_n|\mathbf{x}_{n-1}) &= \mathcal{N}_{\mathbf{x}_n}(\mathbf{G}\,\mathbf{x}_{n-1}, \mathbf{\Gamma}) \\ p(\mathbf{y}_n|\mathbf{x}_n) & \\ &\propto \exp\Big(-\frac{1}{2\sigma_w^2} \sum_{(i,j)\in\mathcal{C}} \big\|\mathbf{A}_{ij,n}\boldsymbol{\vartheta}_{i,n} + \mathbf{B}_{ij,n}\boldsymbol{\vartheta}_{j,n} + \mathbf{a}_d d_{ij,n}\big\|^2\Big). \end{aligned}$$

The global posterior function for all states $\mathbf{x}_1, \ldots, \mathbf{x}_n$ up to n given all observations $\mathbf{y}_1, \ldots, \mathbf{y}_n$ up to n can thus be written as

$$p(\mathbf{x}_1, \ldots, \mathbf{x}_n|\mathbf{y}_1, \ldots, \mathbf{y}_n) \propto p(\mathbf{x}_0) \prod_{m=1}^{n} p(\mathbf{x}_m|\mathbf{x}_{m-1}) p(\mathbf{y}_m|\mathbf{x}_m), \tag{13}$$

where the values $\mathbf{y}_n$ observed for each n are regarded as parameters. The conditional density function for $\mathbf{x}_n$ given all observations $\mathbf{y}_1, \ldots, \mathbf{y}_n$ up to n is the marginal function of (13) given by [19] as

$$\begin{aligned} m_{n|n}(\mathbf{x}_n) &= p(\mathbf{x}_n|\mathbf{y}_1, \ldots, \mathbf{y}_n) \\ &= \int p(\mathbf{x}_1, \ldots, \mathbf{x}_n|\mathbf{y}_1, \ldots, \mathbf{y}_n)\, \mathrm{d}\sim\{\mathbf{x}_n\}, \end{aligned} \tag{14}$$

where $\sim\{\mathbf{x}_n\}$ denotes the integration over all variables except $\mathbf{x}_n$. The mean of $m_{n|n}(\mathbf{x}_n) \propto \mathcal{N}_{\mathbf{x}_n}(\boldsymbol{\mu}_n, \mathbf{\Sigma}_n)$ is the MMSE estimate of $\mathbf{x}_n$ given all observations $\mathbf{y}_1, \ldots, \mathbf{y}_n$ up to n.

We use BP to obtain an efficient computation of (14), which means that we apply message passing over the edges of an FG [19–21]. In general, an FG is a graphical representation of the factorization of a function; for example, the factorization of (13) is illustrated in Fig. 1. Inserting (9) and (11) into (13) allows each vertex $p(\mathbf{y}_n|\mathbf{x}_n)$ to be represented by a subgraph as given in [14], and each vertex $p(\mathbf{x}_n|\mathbf{x}_{n-1})$ by node-independent transitions. For each state $\mathbf{x}_n$, we can thus compute the marginal function $m_{n|n}(\mathbf{x}_{k,n}) \propto \mathcal{N}_{\mathbf{x}_{k,n}}(\boldsymbol{\mu}_{k,n}, \mathbf{\Sigma}_{k,n})$ locally for each state entry $\mathbf{x}_{k,n} \triangleq [\mathbf{x}_n]_k$, which corresponds to the MMSE estimate of either clock parameters $\boldsymbol{\vartheta}_{i,n}$ or a distance $d_{ij,n}$. The resulting FG for BP can be represented graphically by stacking the FG for the posterior function of [14] in discrete-time n and additionally introducing transition functions $p(\mathbf{x}_{k,n}|\mathbf{x}_{k,n-1})$ for each vertex $\mathbf{x}_{k,n}$. Similar to the discussion in [14], disjoint subgraphs of this FG can be related to physical network nodes, which leads to a distributed algorithm.

The message computation rules of BP for a message from a factor vertex f_i to a variable vertex v_i and vice versa are given by [19] as

$$m_{f_i \to v_i}(v_i) \propto \int \zeta(\mathbf{v}) \prod_{v_j \in \mathcal{V}(f_i)\setminus\{v_i\}} m_{v_j \to f_i}(v_j)\, \mathrm{d}\sim\{v_i\}, \tag{15}$$

$$m_{v_i \to f_i}(v_i) \propto \prod_{f_j \in \mathcal{V}(v_i)\setminus\{f_i\}} m_{f_j \to v_i}(v_i), \tag{16}$$

where the function $\zeta(\mathbf{v})$ corresponds to the factor vertex f_i and $\mathbf{v}$ is the vector of all variable vertices (including v_i). The set $\mathcal{V}(f_i)$ holds all adjacent vertices of f_i. Finally, a marginal with respect to a variable v_i, for instance, the marginal function (14), is given by the belief, which is the product over all incoming messages [19]

$$b(v_i) \propto \prod_{f_j \in \mathcal{V}(v_i)} m_{f_j \to v_i}(v_i). \tag{17}$$

Applying (15) and (16) to the previously discussed FG, we compute in a so-called *measurement step* the local outgoing message

$$m_{n|n}(\mathbf{x}_{k,n}) = m_{n|n-1}(\mathbf{x}_{k,n}) \gamma(\mathbf{x}_{k,n}) \tag{18}$$

and in a so-called *prediction step* the local outgoing message

$$\begin{aligned} m_{n|n-1}(\mathbf{x}_{k,n}) &= \int p(\mathbf{x}_{k,n}|\mathbf{x}_{k,n-1}) m_{n|n}(\mathbf{x}_{k,n-1})\, \mathrm{d}\mathbf{x}_{k,n-1} \\ &\propto \mathcal{N}_{\mathbf{x}_{k,n}}(\mathbf{G}\boldsymbol{\mu}_{k,n-1}, \underbrace{\mathbf{G}\mathbf{\Sigma}_{k,n-1}\mathbf{G}^{\mathrm{T}} + \mathbf{\Gamma}}_{\mathbf{P}_{k,n-1}}). \end{aligned} \tag{19}$$

Due to cyclic dependencies between all $\mathbf{x}_{k,n}$, the message $\gamma(\mathbf{x}_{k,n}) = \prod_{f_i \in \mathcal{V}(\mathbf{x}_{k,n})} m^{(M)}_{f_i \to \mathbf{x}_{k,n}}(\mathbf{x}_{k,n})$ is computed iteratively by using M iterations of loopy belief propagation (LBP) in each subgraph representing $p(\mathbf{y}_n|\mathbf{x}_n)$. As presented in [13], each $\mathbf{x}_{k,n}$ therefore needs to compute intrinsic and extrinsic messages, which are exchanged with adjacent vertices $\mathcal{V}(\mathbf{x}_{k,n})$. Since all messages are Gaussian, the parameters of $m^{(m)}_{f_i \to \mathbf{x}_{k,n}}(\mathbf{x}_{k,n}) \propto \mathcal{N}_{\mathbf{x}_{k,n}}(\hat{\boldsymbol{\mu}}^{(m)}_{k,n}, \hat{\mathbf{\Sigma}}^{(m)}_{k,n})$ are computed iteratively in each message-passing period T_m. This leads to the parameter computation rules for $\hat{\boldsymbol{\mu}}^{(m)}_{k,n}$ and $\hat{\mathbf{\Sigma}}^{(m)}_{k,n}$ given by [13] as

$$\big(\hat{\mathbf{\Sigma}}^{(m)}_{k,n}\big)^{-1} = \frac{1}{\sigma_w^2}\Big(\mathbf{V}^{\mathrm{T}}\mathbf{V} - \mathbf{Q}\mathbf{W}^{\mathrm{T}}\mathbf{V}\Big) \tag{20a}$$

$$\big(\hat{\mathbf{\Sigma}}^{(m)}_{k,n}\big)^{-1} \hat{\boldsymbol{\mu}}^{(m)}_{k,n} = -\mathbf{Q}\big(\hat{\mathbf{\Sigma}}^{(m-1)}_{\text{ext}}\big)^{-1} \hat{\boldsymbol{\mu}}^{(m-1)}_{\text{ext}} \tag{20b}$$

with

$$\mathbf{Q} \triangleq \mathbf{V}^{\mathrm{T}}\mathbf{W}\Big(\mathbf{W}^{\mathrm{T}}\mathbf{W} + \sigma_w^2\big(\hat{\mathbf{\Sigma}}^{(m-1)}_{\text{ext}}\big)^{-1}\Big)^{-1}, \tag{21}$$

where the choice of the matrices $\mathbf{V}$, $\mathbf{W}$ depends on the adjacent vertices, and $\hat{\boldsymbol{\mu}}^{(m)}_{\text{ext}}$, $\hat{\mathbf{\Sigma}}^{(m)}_{\text{ext}}$ are parameters of the extrinsic messages, which capture the uncertainty over the parameters from adjacent vertices. Note that the computation of all messages $m_{n|n}(\mathbf{x}_{k,n})$, $m_{n|n-1}(\mathbf{x}_{k,n})$, and $m^{(m)}_{f_i \to \mathbf{x}_{k,n}}(\mathbf{x}_{k,n})$ can be done fully distributed.

Equation (18) can be written explicitly in terms of the parameters $\boldsymbol{\mu}_{k,n}$ and $\mathbf{\Sigma}_{k,n}$ for the message $m_{n|n}(\mathbf{x}_{k,n})$ of an agent node $i \in \mathcal{A}$ as

$$\begin{aligned} &\mathbf{\Sigma}^{-1}_{k,n}\boldsymbol{\mu}_{k,n} = \mathbf{\Sigma}^{-1}_{k,n-1}\mathbf{G}\boldsymbol{\mu}_{k,n-1} \\ &-\sum_{\mathcal{V}(\mathbf{x}_{k,n})} \underbrace{\mathbf{V}^{\mathrm{T}}}_{-\mathbf{H}^{\mathrm{T}}} \Big(\frac{1}{\sigma_w^2} - \frac{1}{\sigma_w^2}\mathbf{W}\mathbf{\Sigma}^{(M)}_{\text{ext}}\mathbf{W}^{\mathrm{T}} \underbrace{\big(\sigma_w^2 + \mathbf{W}\mathbf{\Sigma}^{(M)}_{\text{ext}}\mathbf{W}^{\mathrm{T}}\big)^{-1}}_{\mathbf{\Delta}^{-1}}\Big) \underbrace{\mathbf{W}\boldsymbol{\mu}^{(M)}_{\text{ext}}}_{\mathbf{y}_{i,n}} \end{aligned} \tag{22a}$$

$$\mathbf{\Sigma}^{-1}_{k,n} = \mathbf{P}^{-1}_{k,n-1} + \sum_{\mathcal{V}(\mathbf{x}_{k,n})} \underbrace{\mathbf{V}^{\mathrm{T}}}_{-\mathbf{H}^{\mathrm{T}}} \underbrace{\big(\sigma_w^2 + \mathbf{W}\mathbf{\Sigma}^{(M)}_{\text{ext}}\mathbf{W}^{\mathrm{T}}\big)^{-1}}_{\mathbf{\Delta}^{-1}} \underbrace{\mathbf{V}}_{-\mathbf{H}}. \tag{22b}$$

If the agent node $i \in \mathcal{A}$ has perfect knowledge $\mathbf{\Sigma}^{(M)}_{\text{ext}} \to \mathbf{0}$ of the parameters of node $j \in \mathcal{T}_i$, the terms $\mathbf{\Delta}$ tend to $\mathbf{\Delta} \to \sigma_w^2$ in (22), and (22) is thus equal to the information form of the update equations for Kalman filtering [22, 23] locally on node i. In this case, the local likelihood function of node i can be represented by (8) with $\mathbf{H} = -\mathbf{A}_{ij,n}$ and $\mathbf{y}_{i,n} = \mathbf{B}_{ij,n}\boldsymbol{\vartheta}_{j,n} + \mathbf{a}_d d_{ij,n}$. Hence, the presented distributed filtering algorithm can be interpreted as an iterative approximation to the Kalman filter [19] with a modified measurement noise covariance matrix $\mathbf{\Delta}$ as denoted in (22).

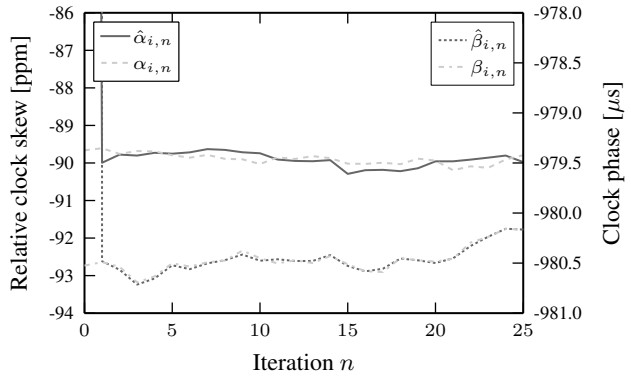

(a) Trend of the estimated clock parameters $\hat{\alpha}_{i,n}$ and $\hat{\beta}_{i,n}$ with respect to the true values $\alpha_{i,n}$ and $\beta_{i,n}$ for a randomly chosen node $i \in \mathcal{A}$.

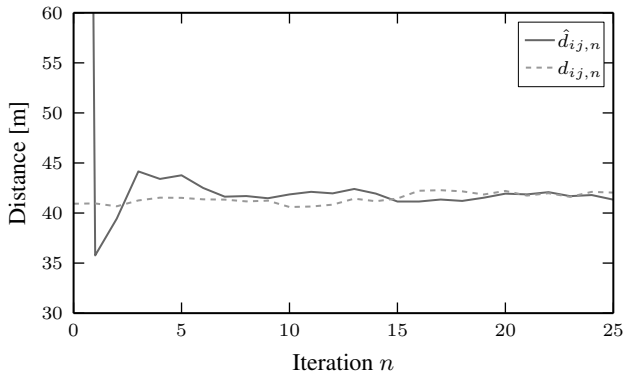

(b) Trend of the estimated distance $\hat{d}_{ij,n}$ with respect to the true distance $d_{ij,n}$ for a randomly chosen pair of nodes $(i,j) \in \mathcal{C}$.

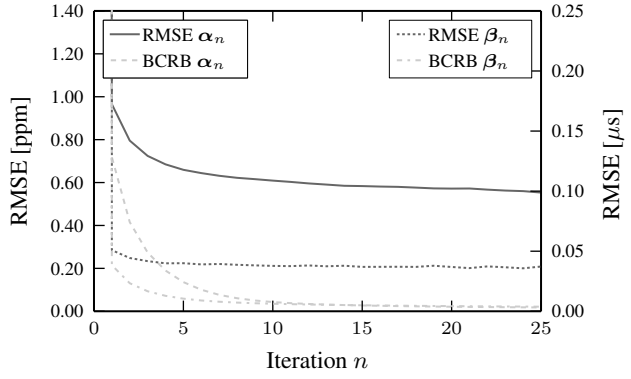

(c) Root mean square errors (RMSEs) of the aggregated clock parameters $\boldsymbol{\alpha}_n$ and $\boldsymbol{\beta}_n$, which are averaged over all nodes $i \in \mathcal{A}$.

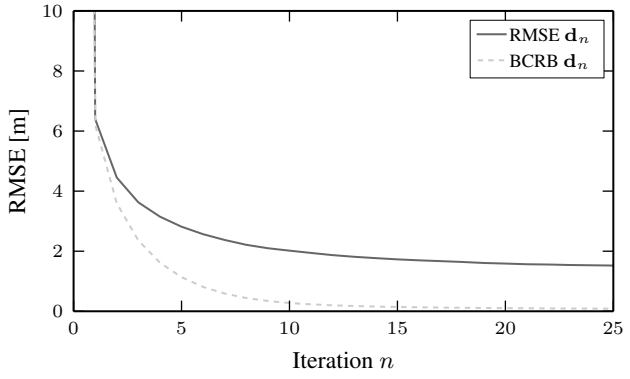

(d) Root mean square error (RMSE) of the aggregated distance $\mathbf{d}_n$, which is averaged over all pairs of nodes $(i,j) \in \mathcal{I}$.

Fig. 2. Simulation results for a random small-world wireless network with $|\mathcal{M}| = 1$ master node and $|\mathcal{A}| = 9$ agent nodes.

5. SIMULATION RESULTS

Our distributed filtering algorithm was simulated on a connected network containing $|\mathcal{M}| = 1$ master node and $|\mathcal{A}| = 9$ agent nodes. Following [24], the network topology was chosen to form a small-world graph, since WNs as a form of spatial graphs tend to be more clustered than random graphs. In every n-th synchronization period T_n of state $\mathbf{x}_n$, all pairs of nodes $(i,j) \in \mathcal{C}$ exchange $K = 10$ measurements and perform $M = 10$ message passing iterations, followed by a state transition to the next state $\mathbf{x}_{n+1}$. The clock skews $\alpha_{i,n}$ were drawn from a uniform distribution with mean 1 and interval length $2 \times 10^{-4} (= \pm 100\,\text{ppm})$, and the phase offsets $\beta_{i,n}$ were drawn from a uniform distribution on the interval $[-1\text{ms}, 1\text{ms}]$. The distances $d_{ij,n}$ were drawn from a uniform distribution on the interval $[1\,\text{m}, R]$, where the communication range was chosen to be $R = 500\,\text{m}$. Finally, the measurement noise standard deviation was $\sigma_w = 93\,\text{ns}$, and the process noise standard deviation was $0.1\,\text{ppm}$, $0.1\,\mu\text{s}$, and $\sqrt{0.1}\,\text{m}$, respectively. The simulation results for 1000 Monte Carlo iterations are illustrated in Fig. 2.

In order to provide a lower bound on the estimation error of our distributed filtering algorithm, the Bayesian Cramér-Rao bound (BCRB) for discrete-time nonlinear filtering was used [25]. In accordance with [26], it can be computed by using message passing on an FG with a structure identical to that shown in Fig. 1. Since the BCRB is computed for Gaussian priors to fulfill the "weak unbiasedness" condition [26], it will always be a lower bound for the estimation error of our distributed filtering algorithm.

6. CONCLUSION

We have presented a distributed filtering algorithm for tracking time-variant clock parameters and internode distances. It can be applied to time-variant WNs, in order to perform cooperative simultaneous ranging and synchronization (CoSRAS). The algorithmic derivation is based on message passing, namely BP, on an FG representing a WN. This leads to efficient local message computation rules for the MMSE estimate of local clock skews and phases of network nodes, as well as of internode distances between neighboring network nodes. Furthermore, we have shown that our fully distributed and decentralized filtering algorithm can be interpreted as a variant of Kalman filtering locally on each node, meaning that it obtains a similar complexity. Simulations, performed on a WN with time-varying clock parameters and distances, provided a frame of reference for the accuracy of the proposed algorithm. In order to provide a lower bound on the estimation error, we computed the corresponding BCRB for nonlinear filtering, which was in the same order of magnitude as the accuracy of our algorithm.

7. REFERENCES

[1] I. F. Akyildiz *et al.*, "A survey on sensor networks," *IEEE Commun. Mag.*, vol. 40, no. 8, pp. 102–114, Aug. 2002.

[2] N. Patwari *et al.*, "Locating the nodes: cooperative localization in wireless sensor networks," *IEEE Signal Process. Mag.*, vol. 22, no. 4, pp. 54–69, Jul. 2005.

[3] G. Antonelli, "Interconnected dynamic systems: An overview on distributed control," *IEEE Control Syst. Mag.*, vol. 33, no. 1, pp. 76–88, Feb. 2013.

[4] O. Hlinka, F. Hlawatsch, and P. M. Djuric, "Distributed particle filtering in agent networks: A survey, classification, and comparison." *IEEE Signal Process. Mag.*, vol. 30, no. 1, pp. 61–81, Jan. 2013.

[5] S. Jagannathan, H. Aghajan, and A. Goldsmith, "The effect of time synchronization errors on the performance of cooperative MISO systems," in *Proc. 2004 IEEE GlobeCom Workshops*, Nov. 2004, pp. 102–107.

[6] G. Antonelli, "Interconnected dynamic systems: An overview on distributed control," *IEEE Control Syst. Mag.*, vol. 33, no. 1, pp. 76–88, Feb. 2013.

[7] Y.-C. Wu, Q. Chaudhari, and E. Serpedin, "Clock synchronization of wireless sensor networks," *IEEE Signal Process. Mag.*, vol. 28, no. 1, pp. 124–138, Dec. 2011.

[8] H.-A. Loeliger, "An introduction to factor graphs," *IEEE Signal Process. Mag.*, vol. 21, no. 1, pp. 28–41, Jan. 2004.

[9] M. Leng and Y.-C. Wu, "Distributed clock synchronization for wireless sensor networks using belief propagation," *IEEE Trans. Signal Process.*, vol. 59, no. 11, pp. 5404–5414, Nov. 2011.

[10] D. W. Allan, "Time and frequency (time-domain) characterization, estimation, and prediction of precision clocks and oscillators," *IEEE Trans. Ultrason., Ferroelectr., Freq. Control*, vol. 34, no. 6, pp. 647–654, Nov. 1987.

[11] J. R. Vig, "Introduction to quartz frequency standards," Army Research Laboratory Electronics and Power Sources Directorate, Tech. Rep. SLCET-TR-92-1, Dec. 1992.

[12] J. Du and Y.-C. Wu, "Fully distributed clock skew and offset estimation in wireless sensor networks," in *Proc. 2013 IEEE Int. Conf. Acoust., Speech, and Signal Process.*, May 2013, pp. 4499–4503.

[13] B. Etzlinger, H. Wymeersch, and A. Springer, "Cooperative synchronization in wireless networks," *IEEE Trans. Signal Process.*, submitted for publication. [Online]. Available: `arXiv:1304.8029 [cs.DC]`

[14] B. Etzlinger *et al.*, "Mean field message passing for cooperative simultaneous ranging and synchronization," in *Proc. 2013 IEEE Global Conf. Signal and Inform. Process.*, Dec. 2013, pp. 583–586.

[15] A. Ahmad *et al.*, "Time-varying clock offset estimation in two-way timing message exchange in wireless sensor networks using factor graphs," in *Proc. 2012 IEEE Int. Conf. Acoust., Speech, and Signal Process.*, Mar. 2012, pp. 3113–3116.

[16] ——, "A factor graph approach to clock offset estimation in wireless sensor networks," *IEEE Trans. Inf. Theory*, vol. 58, no. 7, pp. 4244–4260, Jul. 2012.

[17] ——, "Joint node localization and time-varying clock synchronization in wireless sensor networks," *IEEE Trans. Wireless Commun.*, vol. PP, no. 99, pp. 1–12, Sep. 2013.

[18] M. J. Wainwright and M. I. Jordan, "Graphical models, exponential families, and variational inference," *Foundations and Trends Mach. Learning*, vol. 1, no. 1-2, pp. 1–305, Dec. 2008.

[19] F. R. Kschischang, B. J. Frey, and H.-A. Loeliger, "Factor graphs and the sum-product algorithm," *IEEE Trans. Inf. Theory*, vol. 47, no. 2, pp. 498–519, Feb. 2001.

[20] H.-A. Loeliger *et al.*, "The factor graph approach to model-based signal processing," *Proc. IEEE*, vol. 95, no. 6, pp. 1295–1322, Jun. 2007.

[21] B. J. Frey *et al.*, "Factor graphs and algorithms," in *Proc. 35th Annu. Allerton Conf. Commun., Control, and Computing*, Sep. 1997, pp. 666–680.

[22] R. E. Kalman, "A new approach to linear filtering and prediction problems," *Trans. ASME, J. Basic Eng.*, vol. 82D, pp. 35–45, Mar. 1960.

[23] P. Kaminski, A. E. Bryson, and S. Schmidt, "Discrete square root filtering: A survey of current techniques," *IEEE Trans. Autom. Control*, vol. 16, no. 6, pp. 727–736, Dec. 1971.

[24] A. Helmy, "Small worlds in wireless networks," *IEEE Commun. Lett.*, vol. 7, no. 10, pp. 490–492, Oct. 2003.

[25] P. Tichavsky, C. H. Muravchik, and A. Nehorai, "Posterior Cramér-Rao bounds for discrete-time nonlinear filtering," *IEEE Trans. Signal Process.*, vol. 46, no. 5, pp. 1386–1396, May 1998.

[26] J. Dauwels, "Computing Bayesian Cramér-Rao bounds," in *Proc. 2005 IEEE Int. Symp. Inform. Theory*, Sep. 2005, pp. 425–429.